HHS Public Access

Author manuscript

Exp Eye Res. Author manuscript; available in PMC 2018 August 01.

Published in final edited form as:

Exp Eye Res. 2017 August ; 161: 52–60. doi:10.1016/j.exer.2017.06.005.

Development of wound healing models to study TGFβ3's effect on SMA

Sriniwas Sriram[a,*], **Jennifer A. Tran**[a], **Xiaoqing Guo**[a], **Audrey E.K. Hutcheon**[a], **Andrius Kazlauskas**[b], and **James D. Zieske**[a]

[a]The Schepens Eye Research Institute/Massachusetts Eye and Ear, Department of Ophthalmology, Harvard Medical School, Boston, MA, USA [b]F. Hoffmann-La Roche AG, Basel, Switzerland

Abstract

The goal of this study was to test the efficacy of transforming growth factor beta 3 (TGFβ3) in reducing α- smooth muscle actin (SMA) expression in two models—an ex vivo organ culture and an in vitro 3D cell construct—both of which closely mimic an in vivo environment. For the ex vivo organ culture system, a central 6.0 mm corneal keratectomy was performed on freshly excised rabbit globes The corneas were then excised, segregated into groups treated with 1.0 ng/ml TGFβ1 or β3 (T1 or T3, respectively), and cultured for 2 weeks. The corneas were assessed for levels of haze and analyzed for SMA mRNA levels. For the 3D in vitro model, rabbit corneal fibroblasts (RbCFs) were cultured for 4 weeks on poly-transwell membranes in Eagle's minimum essential media (EMEM) + 10% FBS + 0.5 mM vitamin C ± 0.1 ng/ml T1 or T3. At the end of 4 weeks, the constructs were processed for analysis by indirect-immunofluorescence (IF) and RT-qPCR. The RT-qPCR data showed that SMA mRNA expression in T3 samples for both models was significantly lower ($p < 0.05$) than T1 treatment (around 3-fold in ex vivo and 2-fold in constructs). T3 also reduced the amount of scarring in ex vivo corneas as compared with the T1 samples. IF data from RbCF constructs confirmed that T3-treated samples had up to 4-fold ($p < 0.05$) lower levels of SMA protein expression than samples treated with T1. These results show that T3 when compared to T1 decreases the expression of SMA in both ex vivo organ culture and in vitro 3D cell construct models. Understanding the mechanism of T3's action in these systems and how they differ from simple cell culture models, may potentially help in developing T3 as an anti-scarring therapy.

Keywords

TGFB3; Corneal scarring; PDGF; Ex vivo organ culture; 3D cell culture

[*]Corresponding author. 20 Staniford Street, Boston, MA 02114, USA. Sriniwas_Sriram@meei.harvard.edu (S. Sriram).

Commercial relationship

None (all authors).

1. Introduction

Wound healing in the cornea is unique because anywhere else in the body, an injury would culminate in vascularization and scar formation; however, one of the most crucial aspects of corneal wound healing is how the healing process aims to minimize these end results, which otherwise would lead to serious visual consequences (Gibson et al., 2014; Penn et al., 2012; Sriram et al., 2016).

Corneal wound healing following an injury consists of a series of complex signaling mechanisms controlled by several growth factors, particularly the transforming growth factor beta (TGFβ) family (TGF-β1, -β2, and -β3 or T1, T2, and T3, respectively) (Grazul-Bilska et al., 2003; Jester et al., 2002; Ljubimov and Saghizadeh, 2015). One of the intriguing unanswered questions in this signaling system is how do the highly similar TGFβ isoforms function differently, even though they bind to the same receptors. For instance in some in vivo models, T1 has been shown to be highly fibrotic, while T3 reduced scarring (Pi et al., 2011; Tandon et al., 2010).

In addition to the TGFβ family, there is extensive literature available in different models associating platelet-derived growth factors (PDGFs) and their receptors (PDGFR) to fibrosis(Kaur et al., 2009; Sriram et al., 2017). The PDGF/PDGFR family includes four genes encoding PDGF isoforms (A, B, C, D) and two genes for PDGFR subunits (α and β). Biologically active PDGF is a dimer consisting of one of the following five combinations: AA, AB, BB, CC, and DD. PDGF dimerizes PDGFR subunits into PDGFRα homodimers, PDGFRβ homodimers, or PDGFRαβ heterodimers. The intrinsic affinity of each PDGF isoform for the two PDGFR subunits determines the type of receptor dimer that is assembled (Donovan et al., 2013; Heldin and Westermark, 1990). It has been suggested that TGFβ induces keratocyte proliferation and myofibroblast differentiation through the activation of a PDGF autocrine loop (Jester et al., 2002). Therefore, the difference in T1 and T3's fibrotic activity may be through interactions with PDGF/PDGFR.

In order to better understand the difference in the mechanisms behind T1 and T3's fibrotic activity, we utilized two models in which these mechanisms can be studied in a more isolated environment, a three-dimensional (3D) cell construct model and an ex vivo organ culture model. The 3D construct model, consisted of rabbit corneal fibroblasts cultured for 4 weeks in a stable vitamin C derivative, which allowed the cells to secrete their own extracellular matrix (ECM). Cells in such an environment have been shown to exhibit behavior similar to that of an in vivo system (Karamichos et al., 2010; Ravi et al., 2015). The ex vivo model, consisted of wounded rabbit corneas that were allowed to heal in culture for 2 weeks. It has been shown that ex vivo models for rabbit (Chuck et al., 2001a, 2001b; Sriram et al., 2014; Tanelian and Bisla, 1992) and human corneas (Collin et al., 1995; Janin-Manificat et al., 2012; Kabosova et al., 2003; Saghizadeh et al., 2013) preserved both the histological quality and transparency of the corneas. In addition, corneal scarring attributes observed in vivo systems, such as stromal disorganization, keratocyte proliferation, myofibroblast differentiation, and enhanced provisional extracellular matrix component synthesis, have been reproduced in the ex vivo models (Carrington et al., 2006; Janin-Manificat et al., 2012; Sriram et al., 2014). In this study, the corneal ex vivo model offered

the opportunity to simultaneously look at the effect of T1 or T3 on all three corneal cell types (epithelial, stromal, and endothelial) in their native environment. With the absence of an active immune or nervous system, the wound healing response observed was largely due to the cells response to injury. The organ culture model also ensured high bioavailability of drugs, which can be very difficult to accomplish with in vivo models.

We also examined the idea that TGFβ isoforms exert their differential activity by stimulating different sets of PDGF isoforms. We were particularly interested in PDGFC, a recently identified cytokine that acts via PDGFRα, which we found to be increased in our human 3D cell-culture model following T1 treatment. In addition, PDGFC has been suggested to play an important role in the regulation of fibrosis in different organs, including the heart(Pontén et al., 2003), liver(Campbell et al., 2005), and lung(Zhuo et al., 2006).

To summarize, the main aims of this study were to demonstrate the difference in function between two highly similar TGFβ isoforms—T1 and T3—in two different model systems that closely mimic the in vivo corneal wound healing system. We have also briefly speculated on the mechanism with which T1 and T3 act. We believe the development of these models would lead to a better understanding of T3's role in corneal wound healing and its eventual development as an anti-scarring therapy.

2. Methods

2.1. Cell culture

Cultures of rabbit corneal fibroblasts (RbCFs) were established by outgrowth from rabbit stromal explants, as described previously (Sriram et al., 2013c). Briefly, epithelial and endothelial cells were removed from corneas, the stroma was cut into cubes of approximately 1 mm^3, placed in culture medium consisting of Eagle's Modified Essential Medium (EMEM; American Type Culture Collection [ATCC]; Manassas, VA) supplemented with 10% serum (fetal bovine serum [FBS]: Atlanta Biologicals; Flowery Branch, GA) and an antibiotic-antimycotic cocktail (ABAM; Life Technologies, Carlsbad, CA). Cells from cultures between passages 2 and 5 were used for all experiments.

2.2. 3D construct assembly

Constructs were assembled as previously described (Guo et al., 2007; Karamichos et al., 2011). The RbCFs were plated at a density of 10^6 cells/ml on 6-well plates containing polycarbonate membrane inserts with 0.4 μm pores (Transwell; Corning Costar; Charlotte, NC). RbCFs were cultured for 4 weeks in construct medium—EMEM, 10% FBS, and a stable Vitamin C derivative (VitC: 0.5 mM 2-O-α-D-glucopyranosyl-L-ascorbic acid; Wako Chemicals USA, Richmond, VA). Three groups were tested: (1) Control or C: RbCFs cultured with construct medium; (2) T1: RbCFs grown in construct medium + 0.1 ng/ml T1 (R&D Systems, Inc.; Minneapolis, MN); and (3) T3: RbCFs grown in construct medium + 0.1 ng/ml T3 (R&D Systems). All experiments were performed in triplicate, and constructs were collected and processed for RT-qPCR and indirect immunofluorescence (IF).

2.3. Indirect immunofluorescence

The constructs were collected, fixed, and stained for IF, as previously described (Guo et al., 2007; Karamichos et al., 2011). In brief, after fixation in 4% paraformaldehyde the constructs were incubated overnight at 4 °C with primary antibody against SMA (Dako North America; Carpinteria, CA) in 1% BSA+0.1% Triton-X. The next day, constructs were washed and incubated overnight at 4 °C with the corresponding secondary antibody, anti-mouse IgG (Jackson ImmunoResearch Laboratories, Inc.; West Grove, PA) in 1% BSA +0.1% Triton-X. Iodide counterstain (TO-PRO-3; Life Technologies, Grand Island, NY) was used as a marker of all cell nuclei. Constructs were washed, mounted using Vectashield (Vector Laboratories; Burlingame, CA), observed, and photographed with a confocal microscope (TCS-SP2: Leica Microsystems; Bannockburn, IL).

2.4. Ex vivo organ culture of rabbit corneas

Corneas were cultured as previously described with some important modifications (Castro-Combs et al., 2008; Chuck et al., 2001a; Collin et al., 1995). The ends of 10 ml laboratory test tubes were cut off at the indicator lines nearest to the bottom using a thin saw blade. The cut rims of the tubes were then coated with methyl cyanoacrylate based “super glue” and aseptically pressed onto the center of each well of a 6-well tissue culture plate, creating a dome shaped support surface for the corneas. Plates were then sanitized by placing them under ultraviolet light overnight and then washed with PBS +1% ABAM solution, for 1 h. A 6-mm diameter keratectomy wound of consistent depth was made with a biopsy punch in the central cornea of fresh rabbit globes (Pelfreeze; Rogers, Arkansas). The injured corneas were then surgically dissected from the rabbit globes using a sterile scalpel and forceps, grasping only the scleral rims and not the clear cornea. Test agents were added to the media immediately after the corneas were placed on the domes. The corneas were incubated at 37 °C in a humidified atmosphere containing 5% CO_2 for the duration of the experiment. The culture medium was maintained at the level of the limbal-conjunctival border so that the anterior surface of the cornea was exposed at the air-liquid interface. The entire apparatus was placed on a vertical shaker with gentle movement to moisten the epithelium. At the end of 2 weeks, the central wounded region was dissected and collected for RT-qPCR analysis.

2.5. Scar imaging

The corneal scars were imaged as previously described. (Sriram et al., 2014) Briefly, a Nikon D7000 digital camera was outfitted with a macro lens capable of a native 1:1 reproduction (60 mm Nikkor). The D7000 was set to the “Standard” program, ISO 100, manual exposure with a shutter speed of 1/250 s and f/57. Shutter speed is the amount of time the shutter in the camera remains open. The f-stop value (f/57), or the aperture of the camera, controls how much light can enter the camera (i.e. the smaller the aperture, the smaller the amount of light allowed to enter). To visualize and measure haze, the flash power was set manually (1/6th), and neither the flash nor the lens had a filter. For all images, the lens was set to manual focus and pre-focused to a 1:1 reproduction ratio, and the camera was mounted on a tripod and focused by moving the camera closer or further from the subject. Guide lights on the flash heads were used to facilitate haze visualization and focusing. Due

to the high shutter speed and low aperture, the images were highly reproducible since the influence of background light conditions were significantly reduced.

2.6. Haze grading

The effect of T1 or T3 treatment was manually graded by a method based on a previously published analysis of ex vivo opacity (Janin-Manificat et al., 2012) and the current clinical standard for evaluating corneal scarring. In brief, the corneas were placed in petri dishes filled with PBS and placed over a sheet of paper with printed letters. Three independent observers (blinded to the treatments) manually graded the corneal opacity based on how well they were able to read the letters through the cornea. Scores from 0 to 4 were assigned with 0 being completely transparent—the reviewers were able to read all of the letters—and 4 being the most opaque—the reviewers were unable to read any of the letters.

In addition to the manual grading method, the images of the corneas were also graded using digital image analysis. To improve the contrast of scar formation in the ablated regions of the cornea, the native full color images were converted to gray scale. This was followed by reducing the background light scattering observed in unwounded regions of the cornea to a minimum by setting a color threshold value of 0–43 for all the corneas, using ImageJ software (NIH, v5.2, https://imagej.nih.gov/ij/). All processing steps were performed globally over the entire image, not on any specific area of the image (Sriram et al., 2014; 2013a). These steps help to effectively block the noise associated with the light scattering of unwounded regions, which enables the finer details of the scar to be discerned. The central wounded regions in these processed images were measured, and haze was calculated by measuring the pixel intensity in the selected regions. Percent haze was calculated by normalizing the wounded values to the unwounded corneal values.

2.7. Real time polymerase chain reaction

Total RNA was extracted from both the constructs and the ex vivo tissue samples using Trizol (Life Technologies, CA) according to the manufacturer's directions. Complementary DNA was synthesized using the High Capacity cDNA Reverse Transcription Kit (Applied Biosystems, Carlsbad, CA) according to manufacturer's protocol. The level of mRNA for SMA (Jester et al., 2012), PDGFA, PDGFB, PDGFC, PDGFD and Beta-actin (Choi et al., 2009) was determined by using the Real-Time PCR SYBR Green Assay (KAPA SYBR Fast qPCR master mix: KAPA Biosystems, Wilmington, MA). The primers for each gene were prepared by the CCIB DNA Core Facility at Massachusetts General Hospital (Cambridge, MA) and the sequences are given in Table 1 below. The endogenous control, Beta-actin, was used to normalize target genes. The primers and cDNA were combined with KAPA SYBR Fast qPCR master mix (KAPA Biosystems, Wilmington, MA) and amplification was performed by the Eppendorf Mastercycler ep realplex real-time PCR system (Mastercycler ep realplex real-time PCR system: Eppendorf; Hauppauge, NY). The thermal cycling conditions were as follows: 2 min at 50 °C, 10 min at 95 °C, 40 cycles of 15 s at 95 °C, and 1 min at 60 °C. The relative gene expression of the growth factors was calculated using the $2^{-\Delta\Delta Ct}$ method (Livak and Schmittgen, 2001).

2.8. Statistical analysis

All experiments were performed in triplicate and all statistical analysis was conducted with GraphPad prism (San Diego, CA). Student's t-test or analysis of variances with Tukey's post hoc assessments was accordingly used to test for significant differences between the groups. Results were considered statistically significant when $p < 0.05$.

3. Results

3.1. Comparison of SMA protein and mRNA expression between T1 and T3 treatment in RbCF constructs

To demonstrate the differential effects of T1 and T3 on SMA expression in our 3D construct system, we cultured RbCFs on polycarbonate membrane inserts for a period of 4 weeks. As seen in Fig. 1, RbCF constructs treated with T1 (Fig. 1B) showed a marked increase in SMA expression, as compared with control (Fig. 1A); however, there was no apparent difference noted with T3 treatment (Fig. 1C).

To quantify the data, the constructs were imaged at 2× (Fig. 1A–C, insets), in order to see the whole tissue, and the intensity of SMA staining was then measured with ImageJ software. Fig. 1D shows that SMA intensity was significantly increased ($*p < 0.05$) with T1 treatment (6 fold) when compared with control, whereas, no significant increase was observed with T3 treatment. Fig. 1E shows that SMA mRNA also was significantly increased by T1, as compared with control ($*p < 0.05$, 4 fold), which agrees with the IF data; however, T3 significantly increased SMA mRNA (3 fold) compared to control.

3.2. Comparison of mRNA level expression of PDGF isoforms after T1/T3 treatment in RbCF constructs

To investigate the possibility that TGFβ isoforms exerted their differential activity by each stimulating a different set of PDGF isoforms, we analyzed by RT-qPCR the mRNA expressions of PDGF isoforms collected from RbCF constructs. When compared to the untreated control, T1 treatment significantly increased ($*p < 0.05$) the expression of all the PDGF isoforms; however, there was no significant difference between the control and T3 treatment in any of the PDGF isoforms (Fig. 2).

3.3. Ex vivo organ cultured corneas develop corneal scarring

We wanted to test the effect of T1 or T3 treatment in a model that closely resembled an in vivo system. Corneas from fresh rabbit globes were injured, the corneas were removed, placed on the dome shaped supports in the 6-well plates (Fig. 3A), and media with test agents was added to the limbal-conjunctival border (Fig. 3B). At 14 days after the treatment, haze formation could be clearly observed in the central wounded regions of the wounded-untreated controls (Fig. 4A b). To clearly visualize the amount of scar formation, printed words were placed under the corneas and their legibility was observed (Fig. 4). It can be seen in Fig. 4 that T1 treatment clearly exacerbated scar formation (Fig. 4A c), while T3's effect was less fibrotic (Fig. 4A d). All corneas were visually compared to the unwounded-untreated corneas (Fig. 4A a), which were used as negative controls and showed no signs of corneal scarring.

3.4. Analyzing haze formation using manual grading

We wanted to evaluate the efficacy of treatments using manual haze grading (Fig. 4B and C). On a scale of 0–4, with 0 representing no scar formation and 4 showing the most intense scarring, T1 treatment on average yielded a score of 3.5, and both the wounded- untreated and T3-treated corneas had an average score of 2 (Fig. 4B). The variability of each observation was plotted to account for observer bias (Fig. 4C). T1 treatment significantly produced more scarring than did the wounded-untreated corneas and T3 ($p < 0.5$).

3.5. Analyzing haze formation using digital image analysis

To eliminate the effect of observer bias and to develop a consistent method to evaluate haze formation in ex vivo corneas, we used ImageJ software to perform image analysis. The red pseudo-colored areas in Fig. 5A show the regions picked up under a constant color threshold of 0–43 in all the corneas. The letter “O” located under the central wounded region was consistently used to measure the amount of scar formation in all the corneas. Results from the image analysis (Fig. 5B) showed that T1 treatment increased the amount of scar formation by up to 68%, while the wounded-untreated and T3-treated corneas increased scarring by 45% and 37%, respectively (Fig. 5B). The percent haze values were obtained by normalizing them to unwounded corneas.

We also wanted to test if scar formation in corneas was associated with corresponding changes in SMA mRNA expression (Fig. 5C). We found that wounding and T1 treatment increased SMA expression significantly as compared to unwounded control, ~5 and 6 fold respectively ($p < 0.05$). However, T3 treatment resulted in significantly lower levels of SMA than T1, ~4-fold less ($p < 0.05$:Fig. 5C).

3.6. Comparison of mRNA level expression of PDGF isoforms in ex vivo corneas

To compare the expression of PDGF isoforms after T1 or T3 treatment in both RbCF constructs and ex vivo corneas, we analyzed by RT-qPCR the mRNA expressions of PDGF isoforms from the tissue samples collected from the wounded region of the ex vivo corneas. Similar to the RbCF constructs, T1 treatment significantly increased ($p < 0.05$) the expressions of PDGFA, PDGFC, and PDGFD, while T3 failed to stimulate any of the PDGF isoforms (Fig. 6).

4. Discussion

Studies have shown that blocking T1 (Robinson et al., 2013; Sriram et al., 2013c) (Shah et al., 1992), and in some animals adding exogenous T3 (Shah et al., 1994), (Ferguson et al., 2009), reduces scar formation. However, to date, no regular 2D cell culture model has been able to show a significant difference in function between T1 and T3 (Guo et al., 2016; Wu et al., 1997). Therefore, to examine the difference in T1 and T3’s effect on the expression of SMA, we developed a 3D cell culture model, in which the cells secrete and interact with their own ECM, adding another layer of complexity to regular cell culture experiments. In previous studies, we have shown the anti-fibrotic effect of T3 in a 3D cell culture model consisting of human corneal fibroblasts (HCFs) (Karamichos et al., 2010), and in this study,

we examined the same system using RbCFs. Working with rabbit cells gave us the advantage of extending this study and comparing the effects of T3 in an ex vivo organ culture model.

Using the 3D model, we were able to show that the effect of T3 on SMA mRNA expression was significantly lower than that of T1. In fact, IF resulted in no significant differences in SMA protein expression between T3-treated constructs and untreated controls. This led us to the following two conclusions: 1) T3 was significantly less fibrotic than T1, and 2) It was necessary for the cells to interact with their ECM in order to observe the difference in function between the two TGFβ isoforms.

Although, in vivo models are the ultimate test for a therapy, they also suffer from a number of disadvantages. They are expensive, inconsistent, labor intensive, time consuming, and ultimately ill- suited for exploratory analysis (Foreman et al., 1996), which prompted us to look into ex vivo models. Organ cultures with an air/liquid interface have been shown to have improved epithelial cell morphology, preserved stromal keratocytes, and decreased intercellular edema. Although, there have been a number of re- epithelialization studies on organ culture models (Carrington et al., 2006; Chuck et al., 2001a; Tanelian and Bisla, 1992), there have been very few that have attempted to treat corneal scarring following an injury (Janin-Manificat et al., 2012; Sriram et al., 2013b). Hence, as the next logical step to 3D cell culture models, we developed a physical keratectomy-scarring model for ex vivo organ cultured corneas, and tested the effects of T1 and T3 on fibrosis in this system.

We measured scar formation by both a manual haze-grading method and digital image analysis. Although the manual hazegrading system is the current clinical standard, it suffers from the subjective bias of observers, especially when the efficacies of two different treatments are being evaluated. Hence, the novel digital image analysis method used in this study, which may pave the way toward it's being a standard for ex vivo corneas. Both modes of analysis revealed that T1 increased scar formation following wounding, while T3's effect was significantly less by comparison.

There have been recent studies hypothesizing that the action of T3 may be regulated through PDGFs (Charni Chaabane et al., 2014). Analyzing the expression profiles of PDGF isoforms in ex vivo tissue samples revealed that T1 increased the expression of SMA, PDGFA, PDGFC, and PDGFD isoforms when compared to unwounded controls (Fig. 6). We also observed a similar trend in the 3D cell culture samples, where T1 significantly increased the expression of all PDGF isoforms (Fig. 2). This was not surprising, as T1 has been shown to be a strong mitogen for fibroblasts and to stimulate the expression of a number of pro-fibrotic genes. T3-treated corneas, however, had significantly less SMA expression than wounded- untreated corneas. Interestingly, T3 also failed to stimulate the expression of any of the PDGF isoforms in these corneas. The same trend was observed in the T3-treated 3D construct samples (Figs. 2 and 6). This finding is unique and has never been reported in any of the wound-healing model systems. It is our belief that the difference in function between T1 and T3 stems from the difference in how each stimulates the PDGF isoforms.

Previous studies have shown that SMA immunohistostaining in rabbits after a PTK injury followed a similar pattern of myofibroblast formation as that in ex vivo models (Sriram et

al., 2014). The ease and cost of working with rabbit globes, as opposed to in vivo animals, makes the ex vivo system an ideal model to screen large numbers of potential therapeutic agents. This would also help reduce the need for animals in large drug delivery experiments that require sacrificing animals at regular time points. The air-liquid interface has also been shown to better maintain the cornea's ECM and transparency when compared to submerged models (Marlo et al., 2016).

The drawback of these models, however, is the absence of intact immune systems, lacrimal glands, and corneal innervation, which generates normal inflammatory responses and tear production. Hence, potential treatments identified by this would need to be further tested in vivo in animals.

Although the results are preliminary, we believe T3's relationship with the different PDGF isoforms warrants further study and may be one of the avenues through which T3 decreases its fibrotic activity. To our knowledge, this is the first set of models to successfully show the functional differences between T1 and T3 in the rabbit species, and could pave the way towards using these models to develop future therapies for scarring.

Acknowledgments

Funding

Supported by: NIH/NEI Grant No. EY03790 (Core) and EY005665 (JDZ).

References

Campbell JS, Hughes SD, Gilbertson DG, Palmer TE, Holdren MS, Haran AC, Odell MM, Bauer RL, Ren HP, Haugen HS, Yeh MM, Fausto N. Platelet-derived growth factor C induces liver fibrosis, steatosis, and hepatocellular carcinoma. Proc Natl Acad Sci U S A. 2005; 102:3389–3394. http://dx.doi.org/10.1073/pnas.0409722102. [PubMed: 15728360]

Carrington LM, Albon J, Anderson I, Kamma C, Boulton M. Differential regulation of key stages in early corneal wound healing by TGF-beta isoforms and their inhibitors. Invest Ophthalmol Vis Sci. 2006; 47:1886–1894. http://dx.doi.org/10.1167/iovs.05-0635. [PubMed: 16638995]

Castro-Combs J, Noguera G, Cano M, Yew M, Gehlbach PL, Palmer J, Behrens A. Corneal wound healing is modulated by topical application of amniotic fluid in an ex vivo organ culture model. Exp Eye Res. 2008; 87:56–63. http://dx.doi.org/10.1016/j.exer.2008.04.010. [PubMed: 18555991]

Charni Chaabane S, Coomans de Brachène A, Essaghir A, Velghe A, Re Lo S, Stockis J, Lucas S, Khachigian LM, Huaux F, Demoulin JB. PDGF-D expression is down-regulated by TGFβ in fibroblasts. PLoS One. 2014; 9:e108656. http://dx.doi.org/10.1371/journal.pone.0108656. [PubMed: 25280005]

Choi SI, Kim TI, Kim KS, Kim BY, Ahn SY, Cho HJ, Lee HK, Cho HS, Kim EK. Decreased catalase expression and increased susceptibility to oxidative stress in primary cultured corneal fibroblasts from patients with granular corneal dystrophy type II. Am J Pathol. 2009; 175:248–261. http://dx.doi.org/10.2353/ajpath.2009.081001. [PubMed: 19497990]

Chuck RS, Behrens A, Wellik S, Liaw LLH, Dolorico AMT, Sweet P, Chao LC, Osann KE, McDonnell PJ, Berns MW. Re-epithelialization in cornea organ culture after chemical burns and excimer laser treatment. Arch Ophthalmol. 2001a; 119:1637–1642. 10-1001/pubs.Ophthalmol.-ISSN-0003-9950-119-11-els00062. [PubMed: 11709014]

Chuck RS, Behrens A, Wellik SR, Liaw LH, Sweet PM, Osann KE, McDonnell PJ, Berns MW. Simple organ cornea culture model for re- epithelialization after in vitro excimer laser ablation. Lasers Surg Med. 2001b; 29:288–292. http://dx.doi.org/10.1002/lsm.1121. [PubMed: 11573233]

Collin HB, Anderson JA, Richard NR, Binder PS. In vitro model for corneal wound healing; organ-cultured human corneas. Curr Eye Res. 1995; 14:331–339. [PubMed: 7648858]

Donovan J, Shiwen X, Norman J, Abraham D. Platelet-derived growth factor alpha and beta receptors have overlapping functional activities towards fibroblasts. Fibrogenes Tissue Repair. 2013; 6:10. http://dx.doi.org/10.1186/1755-1536-6-10.

Ferguson MWJ, Duncan J, Bond J, Bush J, Durani P, So K, Taylor L, Chantrey J, Mason T, James G, Laverty H, Occleston NL, Sattar A, Ludlow A, O'kane S. Prophylactic administration of avotermin for improvement of skin scarring: three double-blind, placebo-controlled, phase I/II studies. Lancet. 2009; 373:1264–1274. http://dx.doi.org/10.1016/S0140-6736(09)60322-6. [PubMed: 19362676]

Foreman DM, Pancholi S, Jarvis-Evans J, Mcleod D, Boulton ME. A simple organ culture model for assessing the effects of growth factors on corneal re- epithelialization. Exp Eye Res. 1996; 62:555–564. http://dx.doi.org/10.1006/exer.1996.0065. [PubMed: 8759523]

Gibson DJ, Pi L, Sriram Sriniwas, Mao C, Petersen BE, Scott EW, Leask A, Schultz GS. Conditional knockout of CTGF affects corneal wound healingeffects of conditional CTGF KO in the cornea. Inves Ophthalmol Vis Sci. 2014; 55:2062–2070. http://dx.doi.org/10.1167/iovs.13-12735.

Grazul-Bilska AT, Johnson ML, Bilski JJ, Redmer DA, Reynolds LP, Abdullah A, Abdullah KM. Wound healing: the role of growth factors. Drugs Today. 2003; 39:787–800. [PubMed: 14668934]

Guo X, Hutcheon AEK, Melotti SA, Zieske JD, Trinkaus-Randall V, Ruberti JW. Morphologic characterization of organized extracellular matrix deposition by ascorbic acid-stimulated human corneal fibroblasts. Invest Ophthalmol Vis Sci. 2007; 48:4050–4060. http://dx.doi.org/10.1167/iovs.06-1216. [PubMed: 17724187]

Guo X, Hutcheon AEK, Zieske JD. Molecular insights on the effect of TGF- P1/-P3 in human corneal fibroblasts. Exp Eye Res. 2016; 146:233–241. http://dx.doi.org/10.1016/j.exer.2016.03.011. [PubMed: 26992778]

Heldin CH, Westermark B. Platelet-derived growth factor: mechanism of action and possible in vivo function. Cell Regul. 1990; 1:555–566. [PubMed: 1964089]

Janin-Manificat H, Rovère MR, Galiacy SD, Malecaze F, Hulmes DJS, Moali C, Damour O. Development of ex vivo organ culture models to mimic human corneal scarring. Mol Vis. 2012; 18:2896–2908. [PubMed: 23233791]

Jester JV, Brown D, Pappa A, Vasiliou V. Myofibroblast differentiation modulates keratocyte crystallin protein expression, concentration, and cellular light scattering. Invest Ophthalmol Vis Sci. 2012; 53:770–778. http://dx.doi.org/10.1167/iovs.11-9092. [PubMed: 22247459]

Jester JV, Huang J, Petroll WM, Cavanagh HD. TGFbeta induced myofibroblast differentiation of rabbit keratocytes requires synergistic TGFbeta, PDGF and integrin signaling. Exp Eye Res. 2002; 75:645–657. http://dx.doi.org/10.1006/exer.2002.2066. [PubMed: 12470966]

Kabosova A, Kramerov AA, Aoki AM, Murphy G, Zieske JD, Ljubimov AV. Human diabetic corneas preserve wound healing, basement membrane, integrin and MMP-10 differences from normal corneas in organ culture. Exp Eye Res. 2003; 77:211–217. [PubMed: 12873452]

Karamichos D, Guo XQ, Hutcheon AEK, Zieske JD. Human corneal fibrosis: an in vitro model. Invest Ophthalmol Vis Sci. 2010; 51:1382–1388. http://dx.doi.org/10.1167/iovs.09-3860. [PubMed: 19875671]

Karamichos D, Hutcheon AEK, Zieske JD. Transforming growth factor-β3 regulates assembly of a non-fibrotic matrix in a 3D corneal model. J Tissue Eng Regen Med. 2011; 5:e228–38. http://dx.doi.org/10.1002/term.429. [PubMed: 21604386]

Kaur H, Chaurasia SS, de Medeiros FW, Agrawal V, Salomao MQ, Singh N, Ambati BK, Wilson SE. Corneal stroma PDGF blockade and myofibroblast development. Exp Eye Res. 2009; 88:960–965. http://dx.doi.org/10.1016/j.exer.2008.12.006. [PubMed: 19133260]

Livak KJ, Schmittgen TD. Analysis of relative gene expression data using real-time quantitative PCR and the 2-AACT method. Methods. 2001; 25:402–408. http://dx.doi.org/10.1006/meth.2001.1262. [PubMed: 11846609]

Ljubimov AV, Saghizadeh M. Progress in corneal wound healing. Prog Retin Eye Res. 2015; 49:17–45. http://dx.doi.org/10.1016/j.preteyeres.2015.07.002. [PubMed: 26197361]

Marlo, TL., Giuliano, EA., Sharma, A., Mohan, RR. Development of a novel ex vivo equine corneal model. Vet Ophthalmol. 2016. http://dx.doi.org/10.1111/vop.12415

Penn JW, Grobbelaar AO, Rolfe KJ. The role of the TGF-β family in wound healing, burns and scarring: a review. Int J Burns Trauma. 2012; 2:18–28. [PubMed: 22928164]

Pi L, Xia H, Liu J, Shenoy AK, Hauswirth WW, Scott EW. Role of connective tissue growth factor in the retinal vasculature during development and ischemia. Invest Ophthalmol Vis Sci. 2011; 52:8701–8710. http://dx.doi.org/10.1167/iovs.11-7870. [PubMed: 21969300]

Ponten A, Li X, Thoren P, Aase K, Sjoblom T. Transgenic overexpression of platelet-derived growth factor-C in the mouse heart induces cardiac fibrosis, hypertrophy, and dilated cardiomyopathy. Am J Pathol. 2003 Aug; 163(2):673–682. [PubMed: 12875986]

Ravi M, Paramesh V, Kaviya SR, Anuradha E, Solomon FDP. 3D cell culture systems: advantages and applications. J Cell Physiol. 2015; 230:16–26. http://dx.doi.org/10.1002/jcp.24683. [PubMed: 24912145]

Robinson PM, Chuang TD, Sriram S, Pi L, Luo XP, Petersen BE, Schultz GS. MicroRNA signature in wound healing following excimer laser ablation: role of miR-133b on TGF 1, CTGF, SMA, and COL1A1 expression levels in rabbit corneal fibroblasts. Invest Ophthalmol Vis Sci. 2013; 54:6944–6951. http://dx.doi.org/10.1167/iovs.13-12621. [PubMed: 24065814]

Saghizadeh M, Epifantseva I, Hemmati DM, Ghiam CA, Brunken WJ, Ljubimov AV. Enhanced wound healing, kinase and stem cell marker expression in diabetic organ-cultured human corneas upon MMP-10 and cathepsin F gene silencing. Invest Ophthalmol Vis Sci. 2013; 54:8172–8180. http://dx.doi.org/10.1167/iovs.13-13233. [PubMed: 24255036]

Shah M, Foreman DM, Ferguson MW. Neutralising antibody to TGF-beta 1,2 reduces cutaneous scarring in adult rodents. J Cell Sci. 1994; 107(Pt 5):1137–1157. [PubMed: 7929624]

Shah M, Foreman DM, Ferguson MW. Control of scarring in adult wounds by neutralising antibody to transforming growth factor beta. Lancet. 1992; 339:213–214. [PubMed: 1346175]

Sriram, Sriniwas, Gibson, D., Robinson, P., Tuli, S., Lewin, AS., Schultz, G. Reduction of corneal scarring in rabbits by targeting the TGFB1 pathway with a triple siRNA combination. Adv Biosci Biotechnol. 2013a; 04:55. http://dx.doi.org/10.4236/abb.2013.410A4005.

Sriram, Sriniwas, Gibson, DJ., Robinson, P., Pi, L., Tuli, S., Lewin, AS., Schultz, G. Assessment of anti-scarring therapies in ex vivo organ cultured rabbit corneas. Exp Eye Res. 2014; 125:173–182. http://dx.doi.org/10.1016/j.exer.2014.06.014. [PubMed: 24971495]

Sriram, Sriniwas, Robinson, P., Lewin, A., Schultz, G. Nanoparticle vectored siRNAs reduce profibrotic gene expression in wounded rabbit corneas. ARVO Meet Abstr. 2013b; 54:3878.

Sriram, Sriniwas, Robinson, P., Pi, L., Lewin, AS., Schultz, G. Triple combination of siRNAs targeting TGFβ1, TGFβR2, and CTGF enhances reduction of collagen I and smooth muscle actin in corneal fibroblasts. Invest Ophthalmol Vis Sci. 2013c; 54:8214–8223. http://dx.doi.org/10.1167/iovs.13-12758. [PubMed: 24282226]

Sriram, Sriniwas, Tran, JA., Guo, X., Hutcheon, AEK., Lei, H., Kazlauskas, A., Zieske, JD. PDGFRα Is a Key Regulator of T1 and T3's differential effect on SMA expression in human corneal fibroblasts. Invest Ophthalmol Vis Sci. 2017; 58:1179–1186. http://dx.doi.org/10.1167/iovs.16-20016. [PubMed: 28245298]

Sriram, Sriniwas, Tran, Jennifer A., Zieske, James D. Cornea as a model for testing CTGF-based antiscarring drugs. Bone Tissue Regen Insights Lond. 2016; 7:7–8.

Tandon A, Tovey JCK, Sharma A, Gupta R, Mohan RR. Role of transforming growth factor beta in corneal function, biology and pathology. Curr Mol Med. 2010; 10:565–578. [PubMed: 20642439]

Tanelian DL, Bisla K. A new in vitro corneal preparation to study epithelial wound healing. Invest Ophthalmol Vis Sci. 1992; 33:3024–3028. [PubMed: 1399406]

Wu L, Siddiqui A, Morris DE, Cox DA, Roth SI, Mustoe TA. Transforming growth factor beta 3 (TGF beta 3) accelerates wound healing without alteration of scar prominence. Histologic and competitive reverse-transcription-polymerase chain reaction studies. Arch Surg. 1997; 132:753–760. [PubMed: 9230861]

Zhuo Y, Hoyle GW, Shan B, Levy DR, Lasky JA. Over-expression of PDGF- C using a lung specific promoter results in abnormal lung development. Transgenic Res. 2006; 15:543–555. http://dx.doi.org/10.1007/s11248-006-9007-5. [PubMed: 16830225]

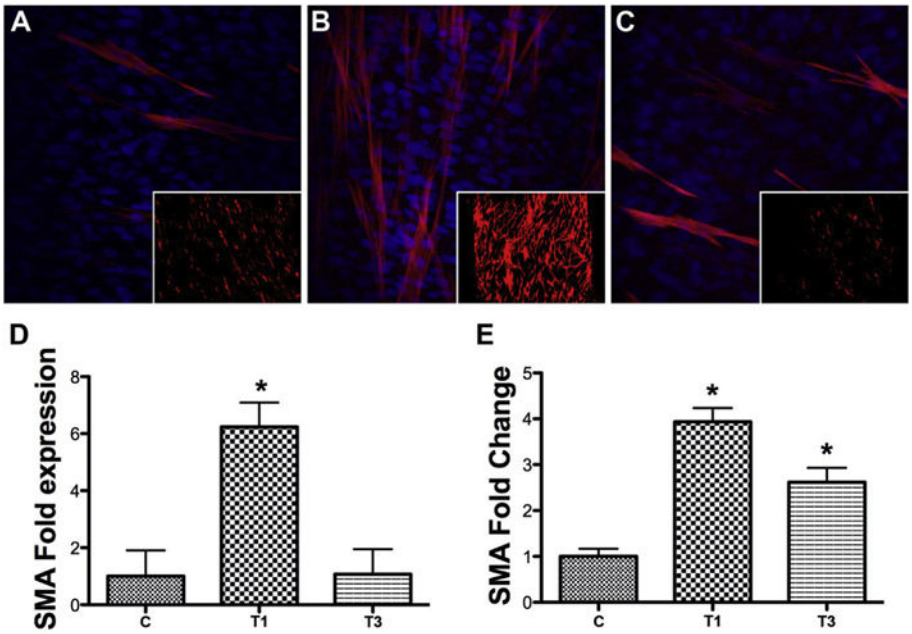

Fig. 1.

SMA localization and expression in 3D RbCF constructs. Representative confocal images of (A) C: untreated control, (B) T1: T1 treated, and (C) T3: T3 treated 3D RbCF constructs at 40× and 2× (insets) stained with anti-SMA (red) and DAPI (blue), a nuclear counterstain. (D) The intensity of the anti-SMA staining in the 2× images was analyzed and the fold enhancement, normalized to the untreated control group (A, inset), was calculated. (E) RT-qPCR was used to analyze SMA mRNA expression in the 3D RbCF constructs, and the fold change was calculated, normalized to the untreated controls. Beta-actin was used as the housekeeping gene. ($n = 3$, $*p < 0.05$). (For interpretation of the references to colour in this figure legend, the reader is referred to the web version of this article.)

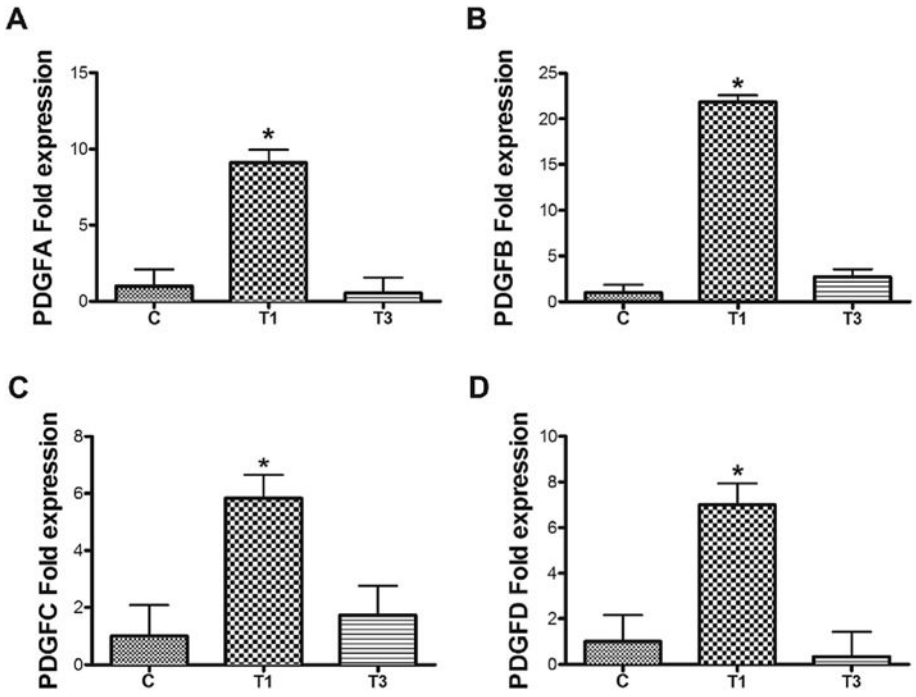

Fig. 2.

Quantification by RT-qPCRof the following PDGF isoforms' mRNA expression: A) PDGFA, B) PDGF B, C) PDGF C, and D) PDGF D from untreated control ("C"), T1-treated ("T1"), and T3-treated ("T3") RbCF 3D constructs. Beta-actin was used as the housekeeping gene. Expression was normalized to the unwounded controls, "C". ($n = 3$, $*p < 0.05$).

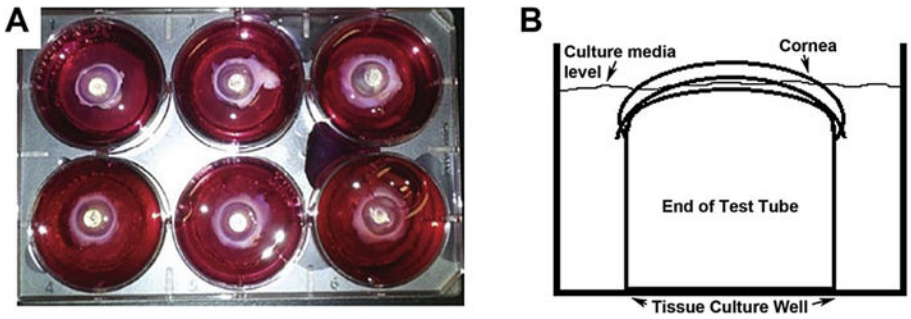

Fig. 3.

Overview of the apparatus used for ex vivo organ culture system. A) Shows a digital image of the ex vivo organ culture model with the corneas in place. B) Shows the schematic of the cell culture system in a lateral view. The end of a l0 ml test tube was placed upside down in a tissue culture well and the corneas were placed over the dome shaped support. The cell culture media was filled to the level of the limbal-conjunctival border so that the anterior surface of the cornea was exposed at the air-liquid interface.

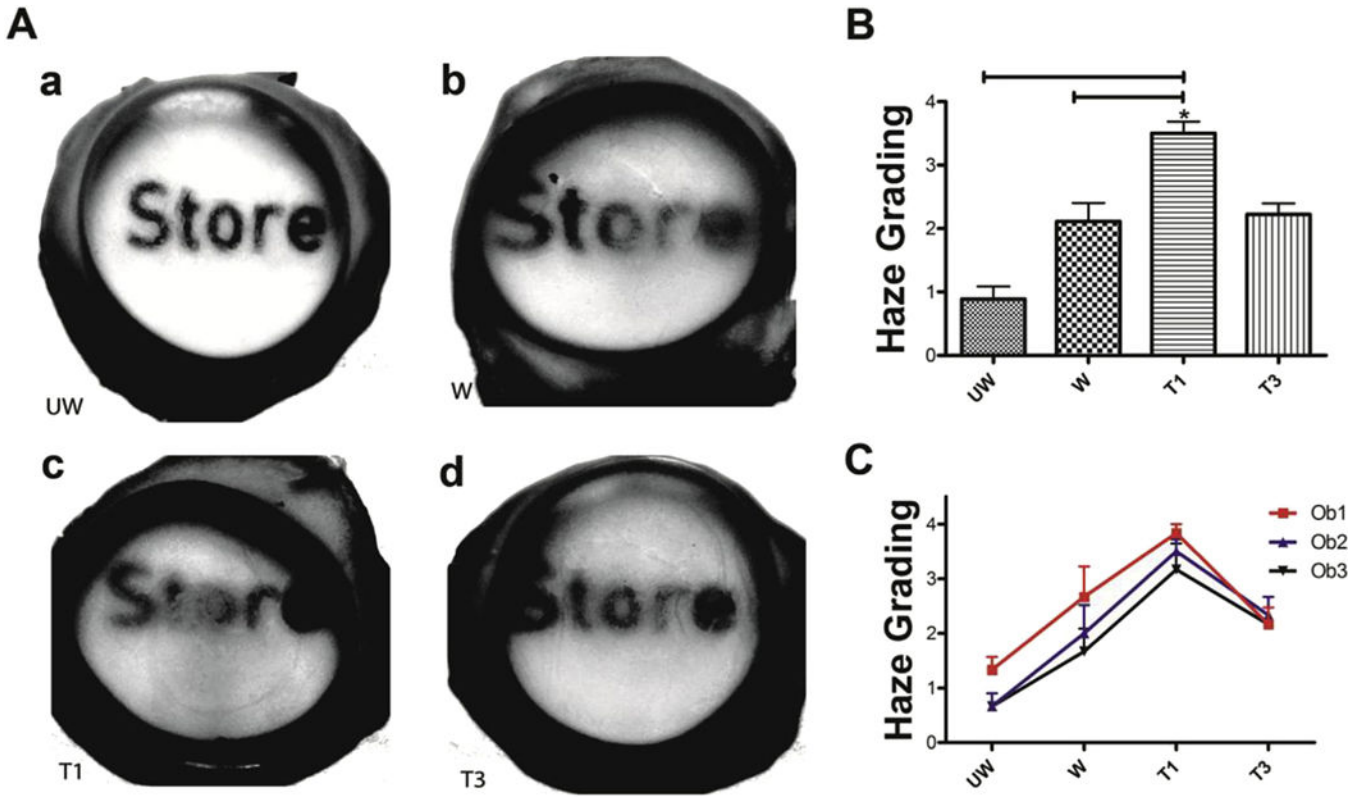

Fig. 4.

Representative visual comparison and manual haze grading of (A.a) UW: unwounded corneas—negative controls, (A.b) W: wounded-untreated corneas—standard for natural scarring, (A.c) T1: wounded-T1-treated, and (A.d) T3: wounded-T3-treated ex vivo corneas. (B and C) Graphs of the manual haze grading of the corneas in (A) as observed by three independent observers blinded to the treatments. On a scale from 0 to 4, with 0 showing no scar formation and 4 showing the most intense scarring. (B) Graph of the average scores of all the observers for each treatment group, and (C) graph of the individual scores of each observer for all the treatment groups. ($n = 3$, $*p < 0.05$).

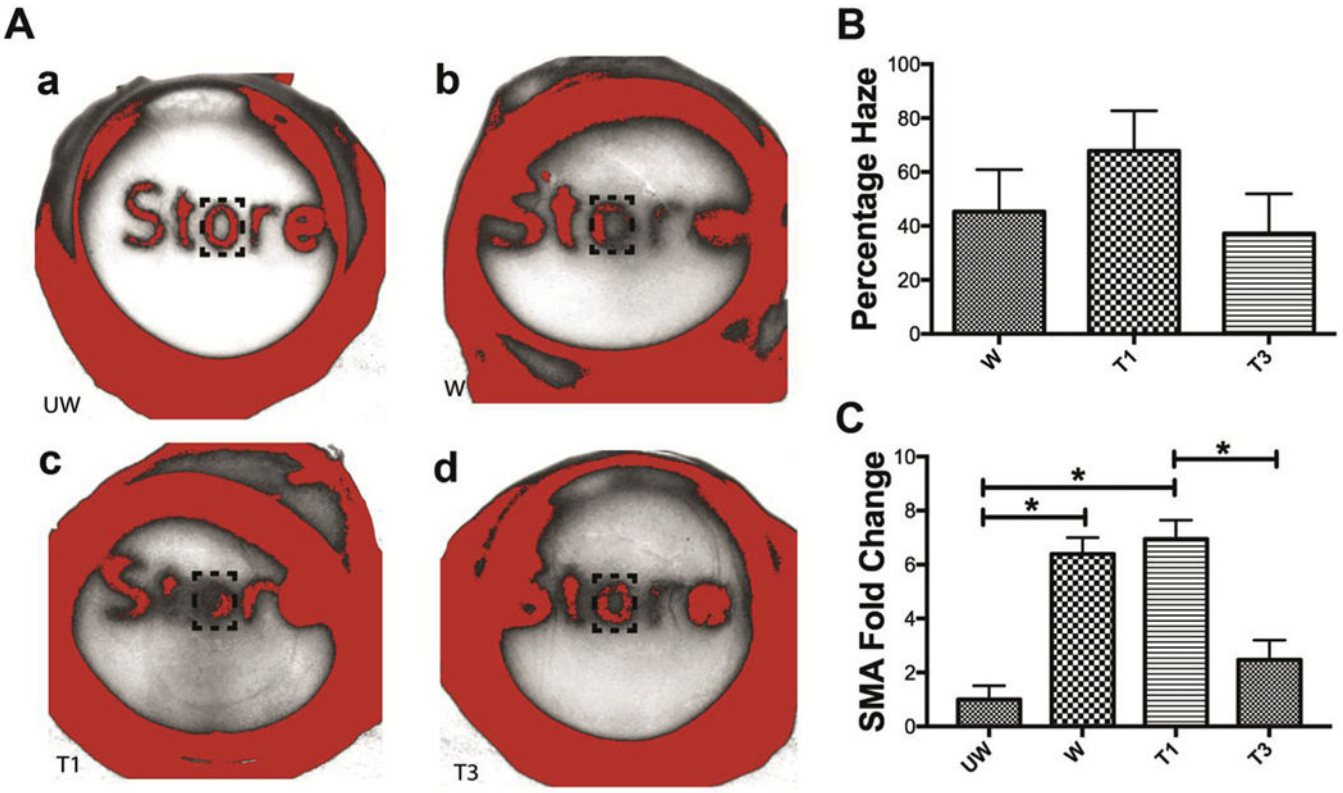

Fig. 5.

Representative visual comparison and digital image analysis haze grading of (A.a) UW: unwounded corneas—negative controls, (A.b) W: wounded-untreated corneas— standard for natural scarring, (A.c) T1: wounded-T1-treated, and (A.d) T3: wounded-T3-treated ex vivo corneas. Images from (A) were analyzed with ImageJ software. The red pseudo-colored areas show the regions picked up under a constant color threshold of 0–43. The letter "O" located under the central wounded region was consistently used to measure the amount of scar formation in all the corneas. (B) Graph of the percent haze as obtained from the analysis of corneas in (A). All values were normalized to unwounded corneas. (C) RT-qPCR analysis of SMA mRNA expression in tissue sections collected from the central wounded region. Beta-actin was used as the housekeeping gene. Expressions were normalized to unwounded controls. ($n = 3$; $p < 0.05$). (For interpretation of the references to colour in this figure legend, the reader is referred to the web version of this article.)

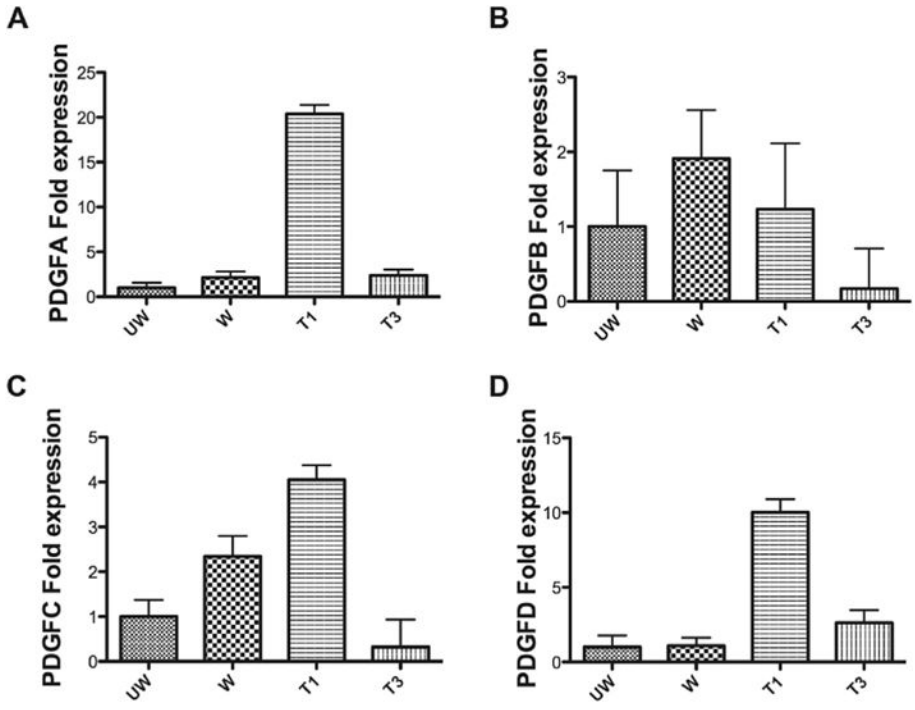

Fig. 6.

Quantification by RT-qPCR of the following PDGF isoforms' mRNA expression: A) PDGF A, B) PDGF B, C) PDGF C, and D) PDGF D from unwounded ("UW"), wounded-untreated ("W"), wounded-T1-treated ("T1"), and wounded-T3-treated ("T3") tissue sections collected from the central region of the ex vivo corneas. Beta-actinwas used as the housekeeping gene. Expression was normalized to the unwounded controls. (n = 3).

Table 1

List of SYBR green primer sequences used for RT-qPCR.

Growth Factor	Forward sequences	Reverse Sequences
SMA	TGCTGTCCCTCTATGCCTCT	GAAGGAATAGCCACGCTCAG
PDGFA	GTGGCCAAGGTGGAGTATGT	CTGAGGCAACCCTGAGGATG
PDGFB	TGGATCTGACCAGGAGGAGG	ATCTTCGTCTCCCGGGTCTC
PDGFC	CTCGCCCCACTCAGCCAAA	ATCTTGTACTCCGTTCTGCTCCTT
PDGFD	CTTTTGTGGAAGATTTCCAGCCT	CAAAGCATCCGCAGTGAGAG
Beta-actin	CGTGCGGGACATCAAGGA	AGGAAGGAGGGCTGGAACA